Coupling of excitons with excitations of the Fermi sea in asymmetric quantum wells

Pawel Hawrylak
Institute for Microstructural Sciences, National Research Council of Canada, Ottawa, Canada K1A 0R6
(Received 26 April 1991)

In asymmetric quantum wells, optical transitions couple a hole state with several conduction-band states. The coupling of excitons associated with higher subbands and free electrons in the lowest subband are investigated using a two-band Mahan–Nozières–De Dominicis Hamiltonian. The emission spectrum for carriers in the lowest subband shows a very weak Fermi edge singularity at the Fermi level. When the Fermi level approaches the second subband, coupling of excitons with excitations of the Fermi sea leads to a large enhancement of the emission spectrum at the Fermi level.

Since the prediction of Mahan[1] of singularities in the x-ray absorption of metals, the problem of optical transitions in the presence of electron gas has been extensively studied.[1] Recent interest has focused on artificially structured materials, in which a quasi-two-dimensional electron gas with a tunable electron density can be created. Good examples are gated heterojunctions,[2] modulation-doped quantum wells,[3–6] and double-barrier resonant-tunneling structures.[7] The presence of the Fermi edge singularity in the emission spectrum involving localized holes has been confirmed by Skolnick *et al.*[3] The ability to engineer samples permits not only the confirmation of known phenomena, but also the investigation of a host of additional effects unknown in bulk materials. Such effects include the coupling of excitons with the excitations of the Fermi sea. The resonant coupling of excitons with excitations of the Fermi sea leads to large changes in optical properties of asymmetric quantum wells, observed recently in light scattering[8] and luminescence[9] experiments. Since the standard perturbation theory based on the summation of an arbitrary class of diagrams (e.g., ladder diagrams) fails completely in the understanding of these phenomena, nonperturbative methods are a necessity. We present here a nonperturbative calculation of the emission spectrum which takes into account the details of the subband structure, screening, excitonic effects, and the shakeup of the Fermi sea for a localized hole in a valence band.

Let us denote the single-particle electron states and energies in the conduction band in the absence of the hole in the valence band by $|k,n\rangle$ and $e_{k,n}$, where k is the wave vector of the plane wave, and n is the subband index. The single-particle states and energies for electrons in the quantum well in the presence of the hole are denoted by $|\lambda\rangle$ and e_λ. The hole potential introduces a mixing of states from different subbands.

Prior to the emission of a photon, the $(N+1)$-electron system in the presence of a hole is in the lowest-energy state $|f\rangle$. The ground state $|f\rangle$ is a product of the Slater determinant of bound and scattering single-particle states $|\lambda\rangle$ and a hole state $|h\rangle$. The stimulated-emission spectrum $E(\omega)$ involves the emission of a photon with frequency ω with simultaneous annihilation of a valence hole and one of the electrons from the conduction band. The annihilation of the hole changes the potential seen by all electrons in the conduction subbands which makes the transition a many-body effect. The emission spectrum $E(\omega)$ is given by a Fourier transform of the real-time current-current correlation function $E(t)$: $E(\omega)=2\,\mathrm{Re}\int_0^\infty dt\, e^{-i\omega t}E(t)$. The current-current correlation function $E(t)$ is given by[10–13]

$$E(t)=\sum_{\lambda,\lambda'} M_\lambda \langle f|e^{iHt}a_\lambda^\dagger c^\dagger e^{-iHt}a_{\lambda'}c|f\rangle M_{\lambda'} . \quad (1)$$

Here $a_\lambda^\dagger$ creates a conduction-band electron in a state $|\lambda\rangle$ with energy e_λ, $c^\dagger$ creates a hole in a state $|h\rangle$ with energy ω_h. The $M_\lambda=P_{vc}\langle\lambda|h\rangle$ is the interband transition matrix element, P_{vc} is an interband momentum matrix element, and $\langle\lambda|h\rangle$ is the overlap between the electron and hole states. The dynamics of the switching off of the hole potential during the emission process is incorporated in the Mahan–Nozières–De Dominicis (MND) Hamiltonian:[1]

$$H=\sum_\lambda e_\lambda a_\lambda^\dagger a_\lambda+(c^\dagger c-1)\sum_{\lambda,\lambda'} V_{\lambda,\lambda'}a_\lambda^\dagger a_{\lambda'}+\omega_h c^\dagger c . \quad (2)$$

The potential $V_{\lambda,\lambda'}$, to be specified later, scatters electrons between different electron states after the hole has vanished. Integrating out the hole degree of freedom in Eq. (1) gives the current-current correlation function $E(t)$ in terms of matrix elements of the final-state Hamiltonian H_f and N-electron states $|\Psi_\lambda\rangle$:

$$E(t)=e^{i\omega_h t}e^{iE_f t}\sum_{\lambda,\lambda'<\mu} M_\lambda\langle\Psi_\lambda|e^{-iH_f t}|\Psi_{\lambda'}\rangle M_{\lambda'} . \quad (3)$$

H_f is the final-state Hamiltonian with a repulsive $(-V)$ hole potential:

$$H_f=\sum_{\lambda,\lambda'}(e_\lambda\delta_{\lambda,\lambda'}-V_{\lambda,\lambda'})a_\lambda^\dagger a_{\lambda'} ,$$

and the electron state $|\Psi_\lambda\rangle$ is a Slater determinant of all occupied states in the Fermi sea except for the state $|\lambda\rangle$. The missing state was annihilated in the emission process. Hence $|\Psi_\lambda\rangle$ describes a hole in the state $|\lambda\rangle$ of the Fermi sea. The energy E_f is the ground-state energy of the

$(N+1)$-electron system in the presence of the hole, and μ is the highest occupied level. As shown by Combescot and Nozières,[10] and Mahan,[3] the current-current correlation function $E(t)$ can be reduced to a closed-form expression involving only the single-particle matrix elements $\phi_{\lambda,\lambda'}$ ($\varphi_{\lambda,\lambda'}=\langle\lambda|e^{-iht}|\lambda'\rangle$, where h is the single-particle Hamiltonian in the absence of the hole):

$$E(t)=e^{i\omega_h t}e^{iE_f t}\det[\phi(t)]\sum_{\lambda,\lambda'<\mu}M_\lambda\phi^{-1}_{\lambda,\lambda'}(t)M_{\lambda'}\ . \quad (4)$$

The matrix ϕ in Eq. (4) is built out of all $N+1$ occupied states in the ground states. The first term in Eq. (4) [$\det(\phi)$] describes the shakeup of the Fermi sea due to the disappearance of the valence hole, while the last term describes vertex corrections, i.e., the scattering of the hole inside the Fermi surface by a repulsive potential in the finite-state Hamiltonian. Note that only occupied electron states contribute to $E(t)$.

The actual calculation of $E(t)$ is nontrivial due to Anderson orthogonality and infrared divergencies, i.e., singularities in the long-time behavior of $E(t)$.[1] This is circumvented by working in the final-state basis $|k,n\rangle$ of plane-wave states in a subband n. We define matrix $G_{k,n,k',n'}$ which describes the propagation of the hole in the Fermi sea in the final-state basis as

$$G_{k,n,k',n'}(t)=\sum_{\lambda,\lambda'<\mu}\langle k,n|\lambda\rangle\phi^{-1}_{\lambda,\lambda'}(t)\langle\lambda'|k',n'\rangle\ ,$$

where $\langle k,n|\lambda\rangle$ are the overlap matrix elements between the initial and final single-particles states. Using the identity

$$\varphi_{\lambda,\lambda'}=\sum_{k,n}\langle\lambda|k,n\rangle e^{-ie_{k,n}t}\langle k,n|\lambda'\rangle\ ,$$

the relationship between the initial matrix elements M_λ and final basis matrix elements $M_{k,n}$ given by $M_\lambda=\sum_{k,n}M_{k,n}\langle\lambda|k,n\rangle$, and the identity $\det(\varphi)=\exp\{\mathrm{Tr}[\ln(\phi)]\}=\exp[-iC(t)]$, a set of *nonlinear* differential equations for the time evolution of the vertex (G) and self-energy (C) functions can be derived:

$$\frac{\partial}{\partial t}G_{k,n,k',n'}(t)=-ie_{k,n}G_{k,n,k',n'}(t)+i\sum_{k'',n''}G_{k,n,k'',n''}(t)\times e_{k'',n''}G_{n'',k'',n',k'}(t)\ , \quad (5)$$

$$\frac{\partial}{\partial t}C(t)=2\sum_{k,n}e_{k,n}G_{k,n,k,n}(t)\ .$$

The relationship between nonlinear differential equations and the edge problem has been pointed out by Schönhammer and Gunnarsson.[14]

The final expression for the current-current correlation function is now given simply in terms of the vertex G and self-energy corrections C:

$$E(t)=e^{iE_f t}e^{i\omega_h t}\sum_{k,n,k',n'}M_{k,n}e^{-iC(t)}e^{+ie_{k,n}t}\times G_{k,n,k',n'}(t)M_{k',n'}\ . \quad (6)$$

An important consequence of working in the final-state basis is that *all* states of the final basis $|k,n\rangle$ contribute to the frequency spectrum of the emission $E(t)$, irrespective of whether they are occupied or empty in the final ground state of the system, i.e., in the absence of the hole. The filling of phase space of initial states enters via the initial condition for matrix $G(0)$:

$$G_{k,n,k',n'}(0)=\sum_{\lambda<\mu}\langle k,n|\lambda\rangle\langle\lambda|k',n'\rangle\ .$$

The overlap matrix elements $\langle k,n|\lambda\rangle$ between the initial and final states are solutions of the Wannier equation:

$$e_{k,n}\langle k,n|\lambda\rangle+\sum_{k',n'}V^{n,n'}_{k,k'}\langle k',n'|\lambda\rangle=e_\lambda\langle k,n|\lambda\rangle\ . \quad (7)$$

Here the attractive electron-hole interaction matrix elements are defined as $V^{n,n'}_{k,k'}=-V(q)F_{n,n'}(q)$, with $q=|k-k'|$ and $V(q)$ the statically screened interaction. $F_{n,n'}$ is a form factor,

$$F_{n,n'}(q)=\int_0^\infty\int_0^\infty\xi_n(z)\xi_{n'}(z)\times\exp(-q|z-z'|)\xi_h^2(z')dz\,dz'\ ,$$

which depends on the position of the hole and subband structure.

In the absence of coupling between different subbands, the eigenstates of Eq. (7) correspond to the bound and scattering excitonic states associated with each individual subband. The only effect of free carriers on the eigenstates of Eq. (7) is the screening of the electron-hole interaction. All subbands contribute irrespective of whether they are occupied or not, and bound states exist for all carrier densities. This is to be contrasted with the rigid Fermi surface approximation where only excitonic states built out of unoccupied states of the initial basis contribute.[6]

The bound exciton state associated with the second subband falls into the continuum of the scattered states of the first subband and turns into a Fano resonance when the intersubband interaction is turned on. The details of the interaction depend on screening and the details of the subband structure of the quantum well.

We calculate the subband structure of an $In_xGa_{1-x}As$ quantum well of thickness w sandwiched by thick layers of $Al_yGa_{1-y}As$ and GaAs. The $Al_yGa_{1-y}As$ layer is doped with silicon, which donates electrons to the well. The subband wave functions $\xi_n(z)$ and energies E_n are obtained by a variational calculation including confining potentials and Hartree energies. The effective potential, the position of energy levels, and wave functions are shown in Fig. 1. The first subband is filled up to the Fermi energy, which is slightly below the bottom of the second subband. The wave function of the first subband peaks close to the $Al_yGa_{1-y}As/In_xGa_{1-x}As$ interface at $z=0$, while the wave function of the second subband has a node at $z=z_0$ and peaks close to the GaAs interface at $z=w$. The schematic wave function ξ_h of the hole localized at z_h is also shown. One expects the hole to be localized at the $In_xGa_{1-x}As/GaAs$ interface due to confining potential and interface defects. Another possibility would be the selective doping with acceptors. For a

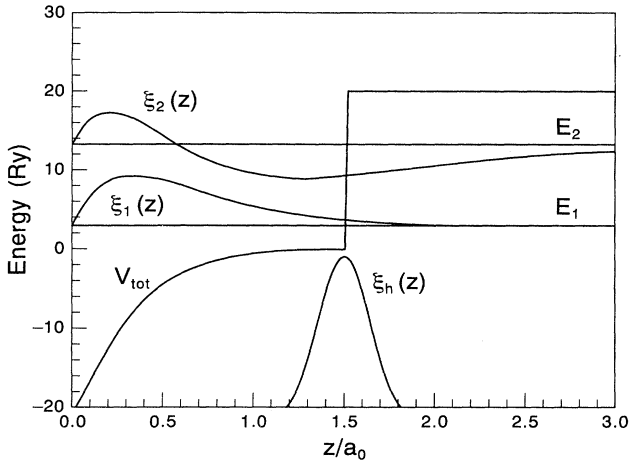

FIG. 1. The subband structure of the asymmetric quantum well. The effective potential, subband wave functions for electrons and holes, and energy levels are shown. Energy is measured in bulk rydbergs (5 meV) and distance in bulk radii (100 Å). The GaAs band offset is 20 Ry, and the thickness of the $In_xGa_{1-x}As$ well is 1.5. These parameters correspond to the sample studied in Ref. 9.

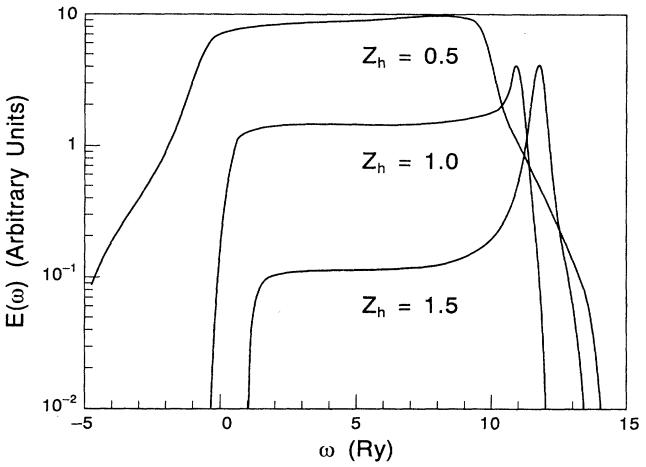

FIG. 3. The changes in the emission spectrum for constant carrier density as a function of the hole position. The change in the position of the hole from $z_h=1.5$ to 0.5 weakens the intersubband excitonic effect.

strongly localized hole at $z=z_h$, the transition matrix elements $M_{k,n}$ can be well approximated by a constant $M_n=M_0,\xi_n(z_h)$, where M_0 is a constant. Hence matrix elements are proportional to the value of the wave function at the hole position.

In Fig. 2 we show the emission spectra as a function of carrier density for the hole localized at the GaAs interface. To underscore the several orders of magnitude changes the scale for the emission intensity is logarithmic. When the Fermi level μ (measured from the bottom of the first subband) is much smaller than the intersubband separation Δ ($\Delta=E_2-E_1$) the emission spectrum

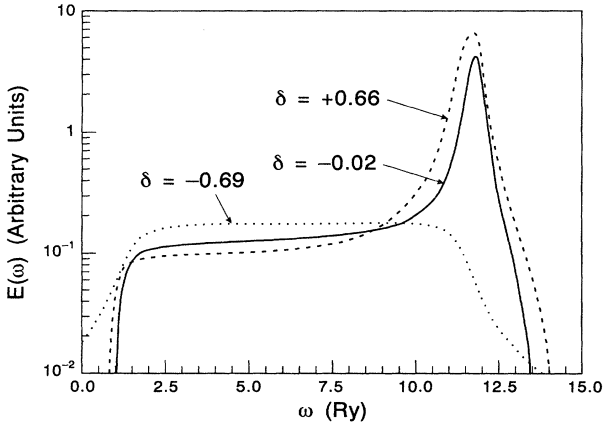

FIG. 2. The enhancement of the emission spectrum $E(\omega)$ from the asymmetric quantum well as the Fermi level crosses the excitonic resonance below the bottom of the second subband. Hole is localized at $z_h=1.5$. The solid line gives enhancement before the second subband becomes occupied.

is basically characterized by the weak Fermi edge singularity as observed in Ref. 3. The singularity arises from the infinitely many low-frequency electron-hole pair excitations of the Fermi sea. As the Fermi level approaches the second subband, in addition to the excitations of the Fermi sea involving electrons and holes in the first subband, there is an increasing contribution from excitations involving holes in the first subband and electrons in the second subband. The second and first subband are strongly mixed by the hole potential in the form of a Fano resonance below the bottom of the second subband. When the Fermi level approaches the second subband, there is a strong interference between the Fermi edge singularity and the excitonic resonance. This is illustrated in Fig. 2, which shows the emission spectrum for three values of the parameter $\delta=\mu-\Delta$: $\delta=-0.69$, $\delta=-0.02$, and $\delta=+0.66$. We see that the emission spectrum in the vicinity of the Fermi edge becomes enhanced (solid line for $\delta=-0.02$) as the Fermi level approaches the second subband, but *before* the second subband becomes populated. The enhancement is large because the overlap of the second subband electron wave function with the valence hole wave function is much larger for electrons in the second subband compared to the first subband. We illustrate the role of matrix elements by localizing the hole in three different positions for fixed carrier density. This changes both the overlap of the electron-hole wave function and effective electron-hole interaction. The emission spectra for different hole positions $z_h=1.5,1.0,0.50$ are shown in Fig. 3. These positions correspond to the following ratio of the second and first subband matrix elements: $M_2/M_1=-4.9,-1.5,+0.16$. As the hole moves toward the center of the well transitions within the first subband begin to dominate and one basically probes the Fermi edge singularity in the first subband. For holes localized at the GaAs interface the intersubband coupling becomes large and enhances the structures at the Fermi level.

In summary, the numerical solution of the multisubband Fermi edge problem in the emission spectrum of modulation-doped quantum wells is presented. Our method allows us to include the coupling of intersubband excitonic transitions with the excitations of the Fermi sea. This coupling is responsible for the enhancement of the Fermi edge singularity in asymmetric quantum wells. Hence optical probes signal the presence of higher subbands when transport measurements would indicate only one subband to be occupied. These results underscore the fact that a photoinjected hole is a large perturbation in the electron system and care must be exercised in comparing optical and transport measurements.

The effects of band-gap renormalization, finite temperature, and finite hole mass will be presented elsewhere.[15]

The author would like to acknowledge useful discussions with A. V. Nurmikko, G. C. Aers, M. W. C. Dharma-wardana, and Jeff Young.

[1]For a review and full references see G. D. Mahan, *Many-Particle Physics* (Plenum, New York, 1981); P. Nozières and C. T. De Dominicis, Phys. Rev. **178**, 1097 (1969); J. Gavoret, P. Nozières, B. Roulet, and M. Combescot, J. Phys. (Paris) **30**, 987 (1969); S. Doniach and M. Šunjic, J. Phys. C **3**, 285 (1970).

[2]C. Delalande, G. Bastard, J. Orgonasi, J. A. Brum, H. W. Liu, and M. Voos, Phys. Rev. Lett. **59**, 2690 (1987).

[3]M. S. Skolnick, J. M. Rorison, K. J. Nash, D. J. Mowbray, P. R. Tapster, S. J. Bass, and A. D. Pitt, Phys. Rev. Lett. **58**, 2130 (1987).

[4]G. Livescu, D. A. D. Miller, D. S. Chemla, M. Ramaswamy, T. Y. Chang, N. Sauer, A. C. Gossard, and J. H. English, IEEE J. Quantum Electron **QE-24**, 1677 (1988).

[5]A. E. Ruckenstein, S. Schmitt-Rink, and R. C. Miller, Phys. Rev. Lett. **56**, 504 (1986).

[6]S. Schmitt-Rink, D. S. Chemla, and D. A. B. Miller, Adv. Phys. **38**, 89 (1989); A. E. Ruckenstein and S. Schmitt-Rink, Phys. Rev. B **35**, 7551 (1987); J. F. Mueller, *ibid.* **42**, 11 189 (1990).

[7]J. F. Young, B. M. Wood, G. C. Aers, R. L. S. Devine, H. C. Liu, D. Landheer, M. Buchanan, A. J. SpringThorpe, and P. Mandeville, Phys. Rev. Lett. **60**, 2085 (1988).

[8]G. Danan, A. Pinczuk, J. P. Vallardes, L. N. Pfeiffer, K. W. West, and C. W. Tu, Phys. Rev. B **39**, 5512 (1989).

[9]W. Chen, M. Fritze, A. V. Nurmikko, D. Ackley, C. Colvard, and H. Lee, Phys. Rev. Lett. **64**, 2434 (1990).

[10]M. Combescot and P. Nozières, J. Phys. (Paris) **32**, 913 (1972).

[11]K. Ohtaka and Y. Tanabe, Phys. Rev. B **39**, 3054 (1989).

[12]T. Uenoyama and L. J. Sham, Phys. Rev. Lett. **65**, 1048 (1990).

[13]G. D. Mahan, Phys. Rev. B **21**, 1421 (1980).

[14]K. Schönhammer and O. Gunnarsson, Phys. Rev. B **18**, 6606 (1978).

[15]P. Hawrylak, Phys. Rev. B **44**, 3821 (1991); (unpublished).